Improved Model of TiO_2 Memristor

Zdenek KOLKA[1], Dalibor BIOLEK[2,3], Viera BIOLKOVA[1]

[1] Dept. of Radio Electronics, Brno University of Technology, Technicka 12, 616 00 Brno, Czech Republic
[2] Dept. of Microelectronics, Brno University of Technology, Technicka 10, 616 00 Brno, Czech Republic
[3] Dept. of Electrical Engineering, University of Defense, Kounicova 65, 662 10 Brno, Czech Republic

kolka@feec.vutbr.cz, dalibor.biolek@unob.cz, biolkova@feec.vutbr.cz

Abstract. *Analysis of Pickett's model of the HP TiO_2 memristor presented in this paper reveals an ambiguity of its port equation, which may cause non-convergence, numerical errors, and non-physical solutions during time-domain simulation. As there is no easy fix of the original model a new behavioral approximation of static I-V characteristics has been proposed. The approximation matches well the original model and is unambiguous.*

Keywords

TiO_2 memristor, Port Equation, State Equation, Pickett's model, simulation

1. Introduction

Resistive switching elements are considered the key components for future memory, logic, and neuromorphic systems [1], [2]. Although the resistive switching phenomenon has been known for a long time, the recognizing memristor in the TiO_2 device manufactured by HP labs in 2008 brought feverish interest in this area [3], [4]. The almost forgotten theory of the "fourth missing element" postulated by L. O. Chua in 1971 came to light to provide a solid theoretical framework for mathematical modeling of memristors [5].

A two-terminal mem-system of the *n*-th order is defined by the following equations [4]

Port Equation (PE): $y(t) = g(\mathbf{x},u,t)u(t)$, (1)

State Equation (SE): $\dot{\mathbf{x}} = f(\mathbf{x},u,t)$ (2)

where $u(t)$ and $y(t)$ represent voltage (v), current (i) or derived quantities like charge (q) and flux (φ); $u(t)$ is the controlling quantity, $y(t)$ is the dependent quantity, and the function g is the generalized response. In the case of memristive systems, (1) relates voltage and current [6]. The internal state of the mem-system is represented by the n-dimensional state vector $\mathbf{x}$, whose evolution is governed by the vector field f. Using formalism (1) and (2), the problem of modeling a memristive system is divided into the modeling of static I-V characteristics (PE) and the modeling of switching dynamics (SE).

The hot topic of current mem-system research is to formulate sufficiently accurate yet simple models for physical devices. The first group of well-known models is based on the concept of linear SE introduced in [3], where the state variable is unbounded. To keep the state variable within physical bounds, the model was later completed with the so-called window functions by Joglekar [7], Biolek [8], Prodromakis [9] and others. These models are popular for their simplicity, easy implementation in SPICE and the possibility of obtaining an analytical solution but, as shown in a comprehensive study [10], they are not able to capture the complex nonlinear behavior of real devices.

The only physical model of the TiO_2 memristor published so far is Pickett's model [11], [12]. The model represents very well both the static characteristics and the switching dynamics but its simulation is sensitive to changes of the excitation signal [10], [13]. Several authors have proposed simpler generic behavioral models that do not exhibit simulation problems and can also be used for other devices. This class includes, for example, models proposed by Laiho [14], Chang [15], and Yakopcic [16]. However, the study [10] points out a possible danger of these models predicting incorrectly the memristor behavior.

The purpose of the present paper is to analyze Pickett's model, whose port equation is ambiguous and this seems to be the origin of non-convergence, numerical errors, and non-physical solutions during time-domain simulation. The paper proposes a modification of the model and an improved behavioral approximation. Section 2 of the paper presents the model analysis and approximation, and Section 3 demonstrates its use.

2. Modeling the HP Memristor

2.1 Pickett's Model and its Anomalous Behavior

The HP memristor is composed of a thin TiO_2 layer between two platinum electrodes. After an electroforming process, most of the oxide is transformed into a highly conductive channel with oxygen vacancies (TiO_{2-X}) except for a nanometer insulating barrier near the positive electrode, see Fig. 1. The barrier width w can be influenced

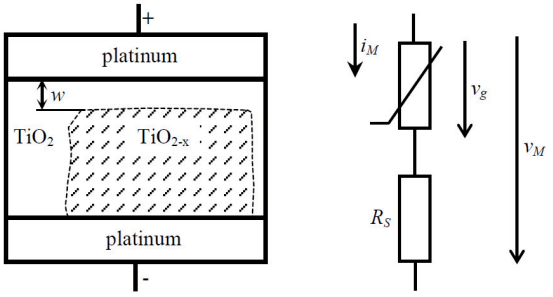

Fig. 1. Cross section of HP TiO_2 memristor and equivalent schematics of the port equation used in Pickett's model [11].

reversibly by a voltage applied across the memristor, causing a dopant drift in the conducting channel. The current flowing through the memristor is determined mainly by the tunneling effect through the narrow barrier, which depends in a highly nonlinear manner on the barrier width [11].

The only physical model of the HP memristor published so far is Pickett's model [11], [12]. Using the memristor modeling formalism (1) and (2), the port equation is represented in an implicit form by a series connection of a resistor R_S and a Metal-Insulator-Metal (MIM) tunneling junction.

The tunneling current is expressed by Simmons's formula for MIM junctions with image forces [17] as a function of the internal voltage v_g and the barrier width w, which is the state variable. The equations read

$$i_M = \frac{\mathrm{sgn}(v_g)\, j}{\Delta w^2} \left\{ \phi_1 \exp\left(-B\Delta w\sqrt{\phi_1}\right) - \left(\phi_1 + e|v_g|\right)\exp\left(-B\Delta w\sqrt{\phi_1 + e|v_g|}\right)\right\} \tag{3}$$

where

$$j = \frac{Ae}{2\pi\hbar},\quad B = \frac{4\pi\sqrt{2m}}{\hbar},\quad \lambda = \frac{e^2\ln(2)}{8\pi\varepsilon_r\varepsilon_0 w}, \tag{4a,b,c}$$

$$w_1 = \frac{1.2\lambda w}{\phi_0},\quad w_2 = w_1 + w\left(1 - \frac{9.2\lambda}{3\phi_0 + 4\lambda - 2e|v_g|}\right), \tag{5a,b}$$

$$\Delta w = w_2 - w_1, \tag{6}$$

$$\phi_1 = \phi_0 - e|v_g|\frac{w_1 + w_2}{2w} - \frac{1.15\lambda w}{\Delta w}\ln\left[\frac{w_2(w - w_1)}{w_1(w - w_2)}\right]. \tag{7}$$

The symbol A represents the junction area, e is the electron charge, m is the electron mass, $\hbar$ is the Planck constant, ε_r is the dielectric constant of the insulator, and ϕ_0 is the barrier height. The variables w_1 and w_2 represent the barrier limits at the Fermi level, and ϕ_1 is the mean barrier height. The numerical constants appearing in (5) and (7) are the result of several approximations introduced by Simmons [17]. The model is symmetric with respect to the applied voltage v_g.

The state equation of Pickett's model reflects the highly asymmetric dynamical behavior for ON switching ($i_M < 0$) and OFF switching ($i_M > 0$) [11]

$$\frac{dw}{dt} = \begin{cases} f_{off}\sinh\left(\dfrac{i_M}{i_{off}}\right)\exp\left(-\exp\left(\dfrac{w - a_{off}}{w_c} - \dfrac{|i_M|}{b}\right) - \dfrac{w}{w_c}\right) & \text{for } i_M \geq 0 \\ f_{on}\sinh\left(\dfrac{i_M}{i_{on}}\right)\exp\left(-\exp\left(\dfrac{a_{on} - w}{w_c} - \dfrac{|i_M|}{b}\right) - \dfrac{w}{w_c}\right) & \text{for } i_M < 0 \end{cases} \tag{8}$$

Parameters f_{on}, f_{off}, i_{on}, i_{off}, a_{on}, a_{off}, b, and w_c in (8) are just fitting parameters without any direct physical meaning.

Paper [11] presents the parameters of Pickett's model identified for a particular TiO_2 memristor. The corresponding i-v characteristic $i_M(v_g)$ of the tunneling barrier alone is plotted in Fig. 2(a) for three different values of w. The curves exhibit negative differential resistance and global activity even for $\Delta w > 0$, which is presented in [12] as the limit of model validity. This behavior does not correspond to the expected characteristics of MIM junctions.

Although the state equation (8) does not impose any explicit limit on w, the boundary values corresponding to the ON and OFF states can be obtained numerically as $w_{on} = 1.23$ nm and $w_{off} = 1.86$ nm for the model parameters published in [12].

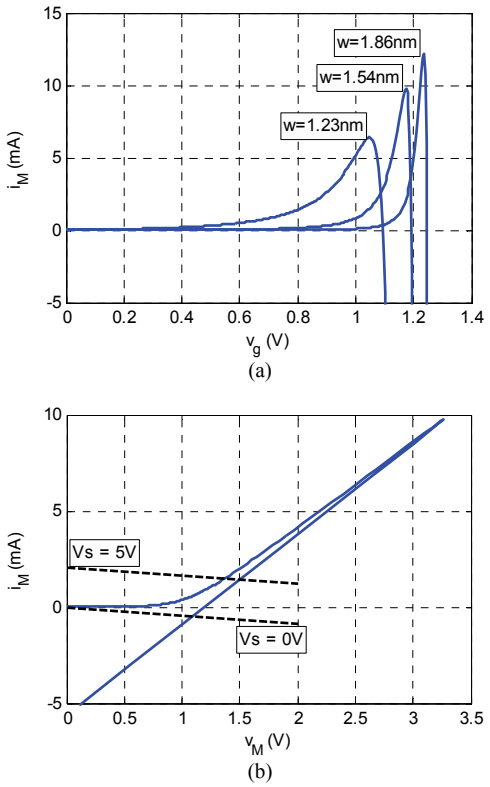

Fig. 2. I-V characteristics of Pickett's model: (a) the tunnel barrier alone; (b) in series with $R_S = 214\ \Omega$ (solid line) drawn for $w = 1.54$ nm.

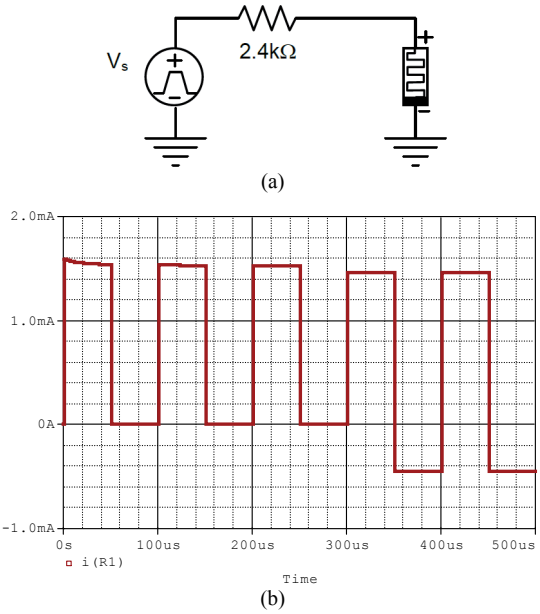

Fig. 3. (a) Reference circuit for simulation; (b) example of incorrect time-domain waveform in PSpice.

Figure 2(b) shows the complete *i-v* characteristic $i_M(v_M)$ including the series resistance $R_S = 214\ \Omega$, see Fig. 1. If the memristor is driven by a DC voltage source V_S with a series resistance of 2.4 kΩ (reference network from [11]), then the circuit admits two solutions, one of which is non-physical. Figure 2(b) also shows (dashed) load lines for the source voltages 0 V and 5 V.

The abrupt nonlinearity of the Port Equation (3) causes convergence problems in the time-domain simulation. Moreover, if simulated without any parasitic capacitance, it is possible that the corrector routine of the time-domain integration method [18] "jumps" to a non-physical solution, an example of which is shown in Fig. 2(b).

The time-domain simulation of the reference circuit with Pickett's model from [11] in PSpice is shown in Fig. 3. The circuit was driven by a rectangular voltage waveform with low level 0 V, high level 5 V, rising and falling times 100 ns, and frequency 10 kHz. The initial condition was $w(0) = 1.228$ nm and the integration step was limited to 35 ns. For the first three periods the low level of current corresponding to $V_s = 0$ V is zero, which is correct. For the last two periods the solution "jumps" to an incorrect negative current, which can also be seen in Fig. 2(b) on the load line for $V_S = 0$ V.

2.2 Modification of Pickett's Model

In the original Simmons's model [17] the quantities w_1 and w_2 represent limits of the potential barrier at the Fermi level. They are given as two real roots of the cubic equation

$$\phi(\chi) = \phi_0 - \frac{ev_g}{w}\chi - \frac{1.15\lambda w^2}{\chi(w-\chi)} = 0, \qquad (9)$$

which lie inside the interval $(0, w)$.

To decrease the complexity and the computational cost, Simmons proposed the following approximate solution:

$$w_1 = \frac{1.2\lambda w}{\phi_0}, \qquad (10a)$$

$$w_2 = w_1 + w\left(1 - \frac{9.2\lambda}{3\phi_0 + 4\lambda - 2e|v_g|}\right), \text{ for } ev_g \le \phi_0 \qquad (10b)$$

and

$$w_1 = \frac{1.2\lambda w}{\phi_0}, \qquad (11a)$$

$$w_2 = (\phi_0 - 5.6\lambda)\frac{w}{ev_g}, \text{ for } ev_g > \phi_0. \qquad (11b)$$

As can be clearly seen, Pickett's model uses only approximation (10) irrespective of the voltage v_g across the barrier. The limiting value of ϕ_0 was identified as 0.95 eV in [11].

Figure 4 compares approximations (10) and (11) with the exact solution of (9). The approximation of w_2 using (10b) differs significantly from the exact solution for $ev_g > \phi_0$, which is the origin of the abrupt nonlinearity in Fig. 2(a).

The transition between (10) and (11) is discontinuous. Therefore the direct use of those formulae in simulation models may bring serious problems both for model parameter identification and for time-domain integration.

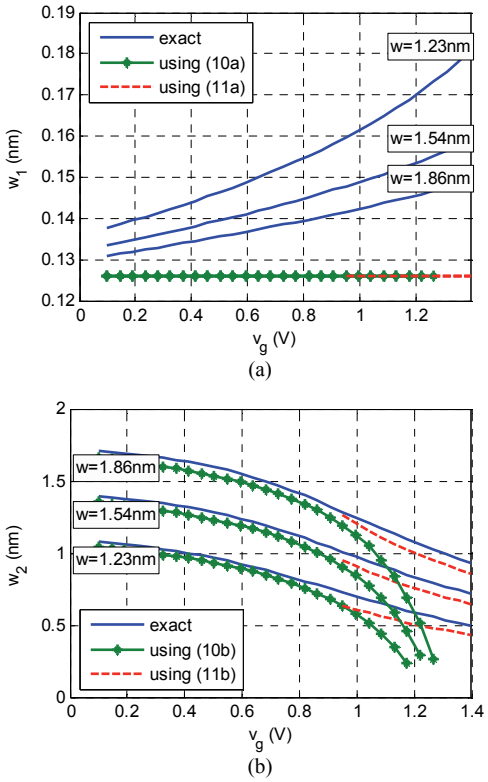

Fig. 4. Comparison of approximate and exact solutions of (9) for (a) w_1 and (b) w_2. Approximation (10b) is plotted intentionally for $v_g > 0.95$ V.

Equation (9) leads to a cubic polynomial with three real roots, which can be solved using Viète's trigonometric substitution

$$a = -w\left(1+\frac{\phi_0}{v_g}\right),\ b = \frac{\phi_0 w^2}{v_g},\ c = -\frac{1.15\lambda w^3}{v_g}, \quad (12a,b,c)$$

$$p = b - \frac{1}{3}a^2,\ q = \frac{2}{27}a^3 - \frac{1}{3}ab + c, \quad (13a,b)$$

$$M = 2\sqrt{-\frac{p}{3}},\ \alpha = \frac{1}{3}\arccos\left(-\frac{q}{2}\sqrt{-\frac{27}{p^3}}\right), \quad (14a,b)$$

$$w_1 = M\cos\left(\alpha+\frac{2\pi}{3}\right)-\frac{a}{3}, \quad (15a)$$

$$w_2 = M\cos\left(\alpha+\frac{4\pi}{3}\right)-\frac{a}{3} \quad (15b)$$

where a, b, c, p, q, M, and α are auxiliary variables to keep the procedure lucid.

The solution is now smooth, but at the cost of computational complexity. In addition, there is an obvious singularity for $v_g = 0$, where (9) leads to only a quadratic equation. The problem can be overcome by forcing some minimal v_g in (12).

2.3 Approximation of Port Equation

The first step of building a behavioral approximation of PE consists in normalizing the barrier width. Let us define a new state variable $x \in [0, 1]$

$$x = \frac{w - w_{on}}{w_{off} - w_{on}}. \quad (16)$$

For $x = 0$ the memristor is in the ON state, which is obtained by long-term application of a negative voltage. On the other hand, the long-term application of a positive voltage brings the memristor to the OFF state with $x = 1$. For the model parameters published in [12] we obtain $w_{on} = 1.23$ nm and $w_{off} = 1.86$ nm.

Figure 5 shows the static nonlinear i-v characteristics of the barrier from [11] for a constant state variable x (negative resistance sections not plotted). For low voltages, i.e. for $|v_g| << \phi_1/e$ the static characteristic can be simplified to [17]

$$i_M = \left(\frac{jBe}{2\Delta w}\sqrt{\phi_1}\ \exp\left(-B\Delta w\sqrt{\phi_1}\right)\right)v_g, \quad (17)$$

which justifies the use of the linear approximation at the origin. As $\Delta w \propto x$ in (17) and with respect to the almost equidistant spacing of individual curves in Fig. 5, the linear memristance R_M in the low-voltage region can be approximated by

$$R_M = R_{on}\left(\frac{R_{off}}{R_{on}}\right)^x \quad (18)$$

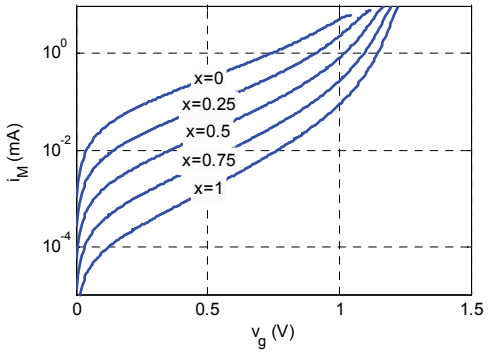

Fig. 5. I-V characteristics of the tunnel barrier for different x.

where R_{on} and R_{off} are memristances for the ON and OFF states, respectively.

The exponential function can be better fitted to experimental characteristics in comparison with the power function proposed in [14], [16], and [19].

The middle region is dominated by the first exponential term in curly brackets in (3), where the applied voltage influences the mean barrier height ϕ_1. Therefore a reasonable approximation is based on the exponential function.

The proposed port equation is based on the modified equation [20]

$$i_M = \mathrm{sgn}(v_g)k_1 k_2^{(1-x)}\left[\sinh\left((k_3+k_4x)|v_g|\right)+k_5\left(\exp\left(k_6|v_g|\right)-1\right)\right] \quad (19)$$

where k_1 to k_6 are fitting parameters. The exponential term with k_5 and k_6 models the region for $v_g > 1$ V.

Neglecting the exponential term, the memristance at the origin, i.e. for $|v_g| << \phi_1/e$, can be obtained as

$$R_M = \frac{1}{d\,i_M/d\,v_g} + R_s, \quad (20)$$

which gives

$$R_{on} = \frac{1}{k_1(k_3+k_4)} + R_s \ \text{ for } x = 1, \quad (21)$$

and

$$R_{off} = \frac{1}{k_1 k_2 k_3} + R_s \ \text{ for } x = 0. \quad (22)$$

For the parameters from [11] the best-fit of (19) gives the following values of parameters: $k_1 = 1.021\times10^{-7}$ A, $k_2 = 438.3$, $k_3 = 5.297$ V^{-1}, $k_4 = 1.608$ V^{-1}, $k_5 = 5.317\times10^{-8}$, $k_6 = 22.35$ V^{-1}. The value of the series resistance R_S was the same as in the original model.

3. Model Evaluation

Figure 6 compares the original static I-V characteristic (3)–(7) with correction (12)–(15) and with approximation (19). The original Pickett's model is considered a reference here as it was fitted to a real device [11]. After correcting w_1 and w_2 in Section 2.2, Simmons's model does not track

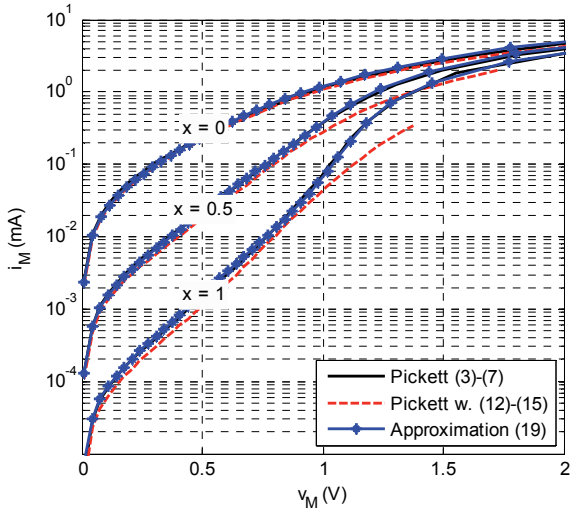

Fig. 6. Comparison of static I-V characteristic of Pickett's model with correction (12)–(15) and approximation (19).

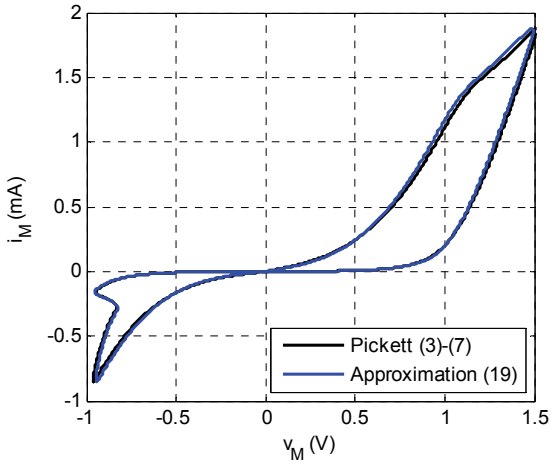

Fig. 7. Comparison of hysteresis loops.

fully the static characteristics near the OFF state for $v_M > 1$ V (dashed curve). On the other hand, the proposed approximation (19) shows a nearly perfect match (dotted curve).

Figure 7 shows a comparison of hysteresis loops between Pickett's reference model and approximation (19). Both models were driven by a 1 kHz harmonic voltage with an amplitude of 4.5 V and a DC component of 1.5 V. The initial condition was $w(0) = 1.228$ nm, i.e. $x = 0$. As can be seen, there is good agreement between the two models.

Acknowledgments

The authors would like to acknowledge the contribution of the EU COST Action IC1401. This work has been supported by the Czech Science Foundation under grant No 14-19865S – Generalized higher-order elements. Research described in this paper was financed by the Czech Ministry of Education in frame of the National Sustainability Program under grant LO1401. For research, infrastructure of the SIX Center was used. The research was also supported by the project FEKT-S-14-2281 and by the Project for the development of K217 Department, UD Brno.

References

[1] YANG, J. J., STRUKOV, D. B., STEWART, D. R. Memristive devices for computing. *Nature Nanotechnology*, 2013, vol. 8, p. 13–24. ISSN: 1748-3387, DOI:10.1038/nnano.2012.240

[2] ADAMATZKY, A., CHUA, L. O. (eds.) *Memristor Networks*. New York (USA): Springer, 2014. ISBN 978-3-319-02630-5

[3] STRUKOV, D. B., SNIDER, G. S., STEWART, D. R., WILLIAMS, R. S. The missing memristor found. *Nature*, 2008, vol. 453, p. 80–83. ISSN: 0028-0836, DOI:10.1038/nature06932

[4] DI VENTRA, M., PERSHIN, Y. V., CHUA, L. O. Circuit elements with memory: Memristors, memcapacitors, and meminductors. *Proceedings of the IEEE*, 2009, vol. 97, no. 10, p. 1717–1724. ISSN: 0018-9219, DOI: 10.1109/JPROC.2009.2021077

[5] CHUA, L. O. Memristor—the missing circuit element. *IEEE Transactions on Circuit Theory*, 1971, vol. 18, no. 5, p. 507–519. ISSN: 0018-9324, DOI: 10.1109/TCT.1971.1083337

[6] BIOLEK, D., BIOLEK, Z., BIOLKOVÁ, V. SPICE Modeling of memristive, memcapacitative and meminductive systems. In *Proc. of the European Conference on Circuit Theory and Design (ECCTD '09)*. Antalya (Turkey), 2009, p. 249–252. ISBN: 978-1-4244-3896-9, DOI: 10.1109/ECCTD.2009.5274934

[7] JOGLEKAR, Y. N., WOLF, S. J. The elusive memristor: properties of basic electrical circuits. *European Journal of Physics*, 2009, vol. 30, no. 4, p. 661–675. DOI: 10.1088/0143-0807/30/4/001

[8] BIOLEK, Z., BIOLEK, D., BIOLKOVÁ, V. SPICE model of memristor with nonlinear dopant drift. *Radioengineering*, 2009, vol. 18, no. 2, p. 210–214. ISSN: 1210-2512 (print)

[9] PRODROMAKIS, T., PEH, B. P., PAPAVASSILIOU, C., TOUMAZOU, C. A versatile memristor model with nonlinear dopant kinetics. *IEEE Transactions on Electron Devices*, 2011, vol. 58, no. 9, p. 3099–3105. ISSN: 0018-9383, DOI: 10.1109/TED.2011.2158004

[10] LINN, E., SIEMON, A., WASER, R., MENZEL, S. Applicability of well-established memristive models for simulations of resistive switching devices. *IEEE Transactions on Circuits and Systems I: Regular Papers*, 2014, vol. 61, no. 8, p. 2402–2410. ISSN: 1549-8328, DOI: 10.1109/TCSI.2014.2332261

[11] PICKETT, M. D., STRUKOV, D. B., BORGHETTI, J. L., YANG, J. J., SNIDER, G. S., STEWART, D. R., WILLIAMS, R. S. Switching dynamics in titanium dioxide memristive devices. *Journal of Applied Physics*, 2009, vol. 106, p. 074508-1–6. ISSN: 0021-8979, DOI: 10.1063/1.3236506

[12] ABDALLA, H., PICKETT, M. D. SPICE modeling of memristors. In *Proc. IEEE International Symposium on Circuits and Systems (ISCAS)*. Rio de Janeiro (Brazil), 2011, p. 1832–1835. ISBN: 978-1-4244-9473-6, DOI: 10.1109/ISCAS.2011.5937942

[13] ASCOLI, A., CORINTO, F., SENGER, V., TETZLAFF, R. Memristor model comparison. *IEEE Circuits and Systems Magazine*, 2013, vol. 13, no. 2, p. 89–105. ISSN: 1531-636X, DOI: 10.1109/MCAS.2013.2256272

[14] LAIHO, M., LEHTONEN, E., RUSSEL, A., DUDEK, P. Memristive synapses are becoming a reality. *The Neuromorhic Engineer*, Nov. 2010, p. 1–3. DOI: 10.2417/1201011.003396

[15] CHANG, T., JO, S.-H., KIM, K.-H., SHERIDAN, P., GABA, S., LU, W. Synaptic behaviors and modeling of a metal oxide memristive device. *Applied Physics A*, 2011, vol. 102, no. 4, p. 857–863. ISSN: 0947-8396, DOI: 10.1007/s00339-011-6296-1

[16] YAKOPCIC, C., TAHA, T. M., SUBRAMANYAM, G., PINO, R. E. Generalized memristive device SPICE model and its application in circuit design. *IEEE Transactions on Computer-Aided Design of Integrated Circuits and Systems*, 2013, vol. 32, no. 8, p. 1201 to 1214. ISSN: 0278-0070, DOI: 10.1109/TCAD.2013.2252057

[17] SIMMONS, J. Electric tunnel effect between dissimilar electrodes separated by a thin insulating film. *Journal of Applied Physics*, 1963, vol. 34, no. 9, p. 2581–2590. ISSN: 0021-8979, DOI: 10.1063/1.1729774

[18] VLACH, J., SINGHAL, K. *Computer Methods for Circuit Analysis and Design.* 2nd edition. New York (USA): Springer, 1993. ISBN: 0897895967

[19] LEHTONEN, E., LAIHO, M. CNN using memristors for neighbourhood connections. In *Proc. of 12th International Workshop on Cellular Nanoscale Networks and Their Applications (CNNA)*. Berkeley (USA), 2010, p. 1–4. ISBN: 978-1-4244-6679-5, DOI: 10.1109/CNNA.2010.5430304

[20] YANG, J. J., PICKETT, M. D., LI, X., OHLBERG, D. A. A., STEWART, D. R., WILLIAMS, R. S. Memristive switching mechanism for metal/oxide/metal nanodevices. *Nature Nanotechnology*, 2008, vol. 3, p. 429–433. ISSN: 1748-3387, DOI: 10.1038/nnano.2008.160

About the Authors ...

Zdeněk KOLKA received the MSc degree in 1992 and the Ph.D. degree in 1997, both in Electrical Engineering, from Brno University of Technology (BUT), Czech Republic. In 1995, he joined the Dept. of Radio Electronics, Brno University of Technology. His scientific activity is directed to the areas of general circuit theory, computer simulation of electronic systems and digital circuits. For years, he has been engaged in algorithms of the symbolic and numerical computer analyses of electronic circuits. He has published over 100 papers. At present, he is a professor at BUT in the field of Radio Electronics.

Dalibor BIOLEK – for the CV see page 377 of this Issue.

Viera BIOLKOVÁ – for the CV see page 377 of this Issue.